ISSN 2464-4617 (print)
ISSN 2464-4625 (online)
Computer Science Research Notes - CSRN 3301
http://www.wscg.eu
WSCG 2023 Proceedings

Low-Rank Rational Approximation of Natural Trochoid Parameterizations

Csaba Bálint
Eötvös Loránd University
1/C Pázmány Péter stny.
1117 Budapest, Hungary
csabix@inf.elte.hu

Gábor Valasek
Eötvös Loránd University
1/C Pázmány Péter stny.
1117 Budapest, Hungary
valasek@inf.elte.hu

Lajos Gergó
Eötvös Loránd University
1/C Pázmány Péter stny.
1117 Budapest, Hungary
gergo@inf.elte.hu

ABSTRACT

Arc-length or natural parametrization of curves traverses the shape with unit speed, enabling uniform sampling and straightforward manipulation of functions defined on the geometry. However, Farouki and Sakkalis proved that it is impossible to parametrize a plane or space curve as a rational polynomial of its arc-length, except for the straight line. Nonetheless, it is possible to obtain approximate natural parameterizations that are exact up to any epsilon. If the given family of curves possesses a small number of scalar degrees of freedom, this results in simple approximation formulae applicable in high-performance scenarios. To demonstrate this, we consider the problem of finding the natural parametrization of ellipses and cycloids. This requires the inversion of elliptic integrals of the second kind. To this end, we formulate a two-dimensional approximation problem based on machine-epsilon exact Chebhysev proxies for the exact solutions. We also derive approximate low-rank and low-degree rational natural parametrizations via singular value decomposition. The resulting formulae have minimal memory and computational footprint, making them ideal for computer graphics applications.

Keywords

Curves, Approximation, Arc-length parametrization, Natural parametrization

1 INTRODUCTION AND PREVIOUS WORK

The parametrization of a curve is not unique since there are infinitely many variations that result in the same shape. However, the analytic derivatives of the curve do change in the process. Natural or arc-length parametrization stands out in the sense that the artifacts of parametrization are absent from the algebraic formulation of derivatives. In other words, the derivatives of an arc-length parametrized curve only consist of geometric invariants, such as curvature and torsion, and their derivatives. This is a direct consequence of the Frenet-Serret formulae [Car18].

Unfortunately, natural parametrization is not a feasible practical representation. This was first proven rigorously by Farouki and Sakkalis [FS07] when they showed that no plane or space curve may be parametrized as a rational polynomial function of its arc-length, except for the line. However, they have identified a subset of polynomials that possess polynomial arc-length functions. This class of polynomials is referred to as Pythagorean hodographs. Although it is still not possible to parametrize these by arc-length, the ability to express the arc-length in closed form proved to be of merit in various applications [Far08].

Nonetheless, approximate arc-length parametrizations may offer practical alternatives. Farouki considered the Möbius transformation to reparametrize degree n Bézier curves such that the result is approximately unit speed [Far97]. He showed that there is a unique reparametrization of this kind that minimizes a functional that penalizes deviation from unit speed traversal. A more elementary derivation to this result was given by Jüttler in [Jüt97].

Sánchez-Reyes and Chacón proposed an approximate arc-length parametrization of plane curves in [SC15] that does not rely on optimization. They constructed second-order geometric Hermite interpolants [BHS87] to approximate an arbitrary input curve. Quintic polynomials are capable of reconstructing both geometric invariants and parameterization up to second order at endpoints [Sch98]. The latter were chosen such that the interpolant is unit-speed and possesses orthogonal first and second derivatives, while the former was used to reconstruct position, tangent, and curvature centers at the parametric endpoints. To achieve the desired accuracy, they employed multiple geometric Hermite segments.

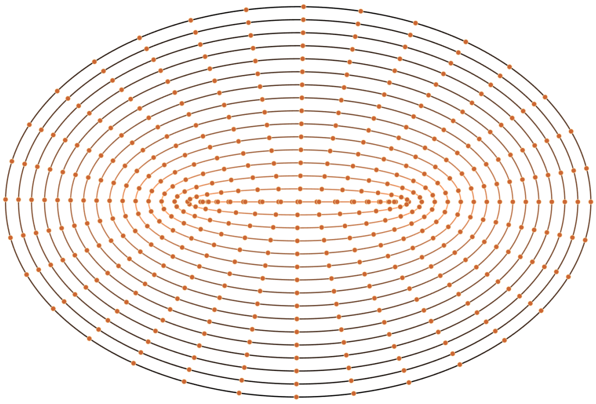

(a) Parameterization from Equation (1)

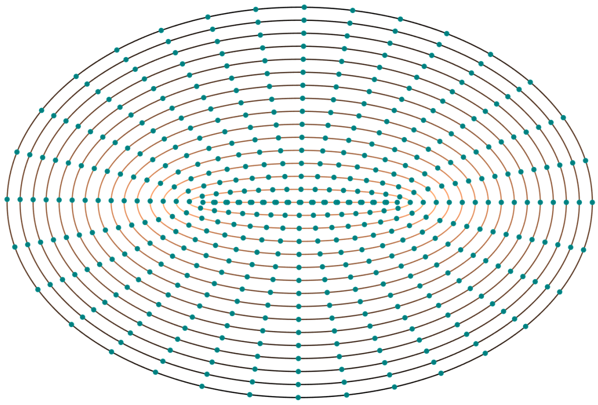

(b) Natural ellipse parameterization.

Figure 1: Ellipse and its natural parameterization

We also consider the problem of approximating arc-length parametrizations; however, we focus our attention on adjustable precision and restrict our discussion to trochoid curves only. To this end, we present a scaleable framework that may be used to devise high-accuracy approximate natural parametrizations of trochoids by means of rational approximations.

In Section 2, we briefly review how an incomplete elliptic integral of the second kind is derived upon formulating the natural parametrization of ellipses and trochoids and what simplifications can be applied to it.

In Section 3, we show that a low-rank separable approximation may be computed from a properly sampled simplified formulation, and Section 4 shows that it can be realized by custom degree rational polynomials.

We show that even degree $(2,1)$ rational polynomial separable approximations yield high accuracy results with negligible computational cost in Section 5.

2 APPROXIMATE NATURAL PARAMETERIZATIONS

There are various means to approximate the arc-length parametrization of a curve. Methods such as Runge-Kutta provide procedural solutions; however, our aim is to derive closed-form approximations.

Let us consider how the natural parameterization of an ellipse with semi-major axis a and semi-minor axis b is derived. A general parametrization is given as

$$\boldsymbol{p}(\phi) = \begin{bmatrix} a\cos(\phi) \\ b\sin(\phi) \end{bmatrix} \ , \ \ \phi \in [0, 2\pi),\ 0 < b < a \in \mathbb{R}\ . \quad (1)$$

From Equation (1), the arc-length function is

$$\begin{aligned} s_{\boldsymbol{p}}(\phi) &= \int_0^\phi \sqrt{a^2 \sin^2 \varphi + b^2 \cos^2 \varphi}\, \mathrm{d}\varphi \\ &= b \cdot \int_0^\phi \sqrt{1 - \left(1 - \tfrac{a^2}{b^2}\right) \cdot \sin^2 \varphi}\, \mathrm{d}\varphi\ . \end{aligned}$$

Thus, we can express the arc-length function with the incomplete elliptic integral of the second kind, denoted as $\mathrm{E}(\phi|m)$. Inverting this and substituting back to Equation (1) leads to the natural parameterization of the ellipse:

$$\begin{aligned} s_{\boldsymbol{p}}(\phi) = b \cdot \mathrm{E}\left(\phi \,\middle|\, 1 - \tfrac{a^2}{b^2}\right) \implies \\ \boldsymbol{p}\left(s_{\boldsymbol{p}}^{-1}(s)\right) = \boldsymbol{p}\left(\mathrm{E}^{-1}\left(\tfrac{s}{b} \,\middle|\, 1 - \tfrac{a^2}{b^2}\right)\right)\ . \end{aligned}$$

2.1 Trochoid parameterization

The following trochoid parameterization unifies hypotrochoids and epitrohods while also describing circles, ellipses, hypocycloids, and epicycloids with only two parameters:

$$\boldsymbol{p}(\phi) = \begin{bmatrix} \cos\phi + a\cos(b\phi) \\ \sin\phi + a\sin(b\phi) \end{bmatrix} \ , \ a, b \in \mathbb{R} \setminus \{0\}\ . \quad (2)$$

Note that if $a = 0$ or $b = 0$ or $b = 1$, the curve is just a circle. When $b = -1$, the above simplifies to an equation of an ellipse with $a+1$ semi-major axis and $1-a$ semi-minor axis. Observe that the curves

$$\boldsymbol{p}_{a,b}(\phi),\ \boldsymbol{p}_{-a,b}(\phi),\ \boldsymbol{p}_{a,\frac{1}{b}}(\phi),\ \boldsymbol{p}_{-a,\frac{1}{b}}(\phi)$$

only differ in scale and rotation from each other. Thus, without the loss of generality, we can assume that $a > 0$ and $0 \neq b \in [-1, 1]$.

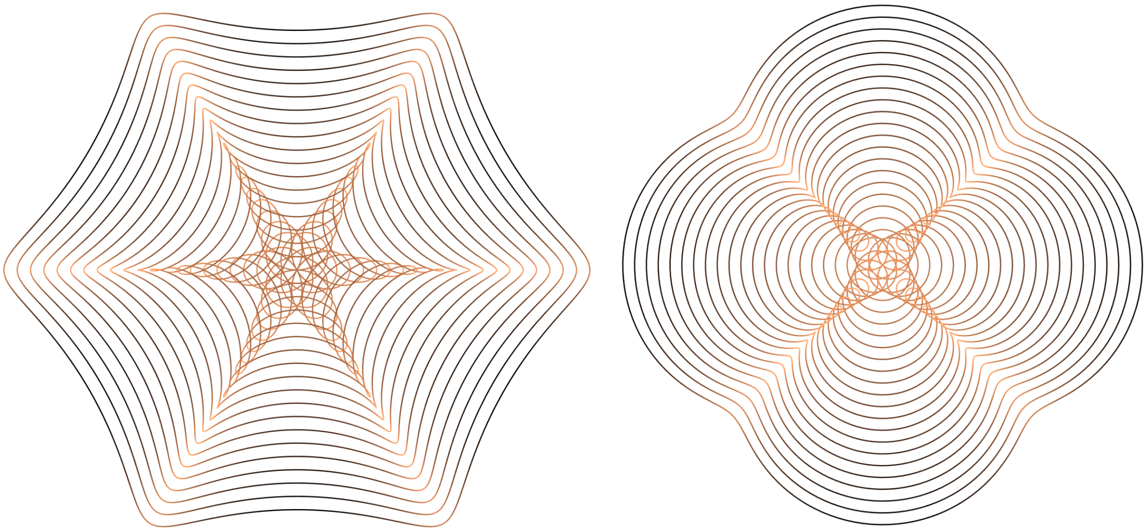

(a) Epitrochoids with $b = \frac{1}{5}$.

(b) Hypotrochoids with $b = -\frac{1}{5}$.

Figure 2: Trochoids with different values of a from Equation (2).

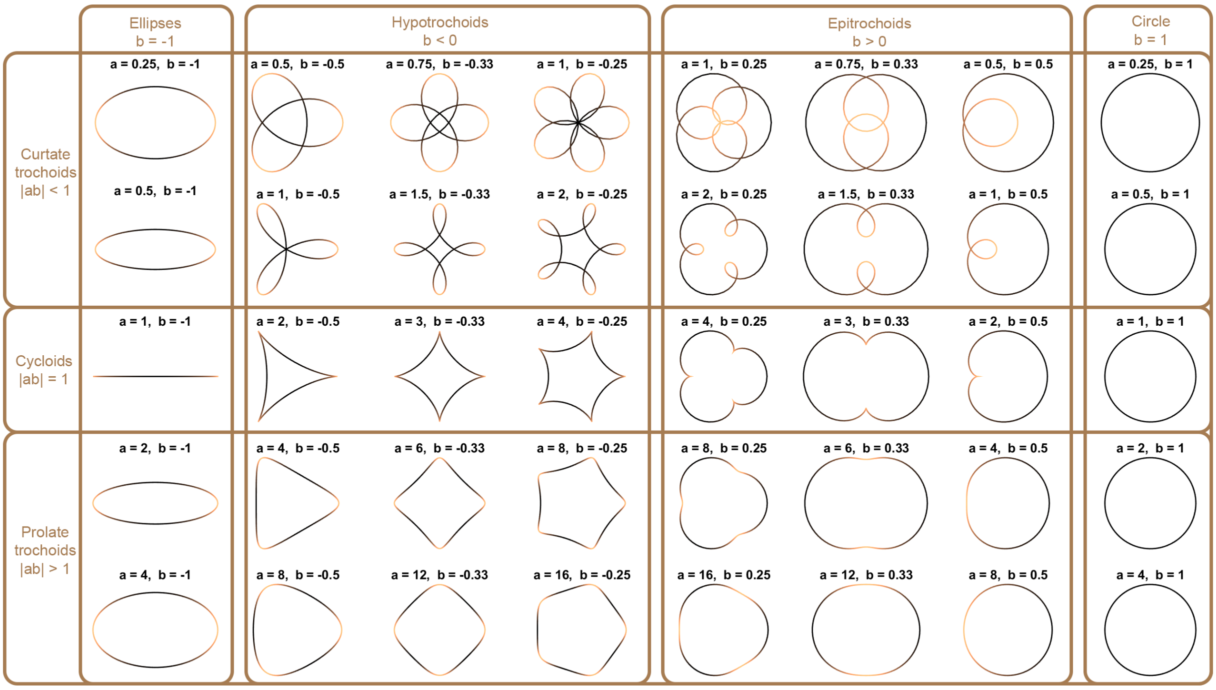

Figure 3: Classification of the trochoid curve family with Equation (2).

Table 1 and Figure 3 classify these trochoids, so we can relate Equation (2) to the well-known constructive derivation via rotating circles.

A wide range of plane curves fall into this categorization, such as the Tusi couple ($a = 1, b = -1$) that creates linear motion from rotational one. The cardioid ($a = 2, b = \frac{1}{2}$) that appears in our coffee cups or the deltoid curve $a = 2, b = -\frac{1}{2}$, limaçon curves $b = \frac{1}{2}$, the nephroid $a = 3, b = \frac{1}{3}$, the astroid $a = 3, b = -\frac{1}{3}$, and cycloids in general $|ab| = 1$ including the tautochrone and the brachistochrone curves.

We obtain the arc-length parameterization of trochoids similarly to ellipses:

$$\begin{aligned}
s_{\boldsymbol{p}}(\phi) &= \int_0^\phi \sqrt{a^2b^2 + 2ab\cdot\cos((b-1)\varphi)}\,\mathrm{d}\varphi \\
&= \int_0^\phi \sqrt{(1+ab)^2 - 4ab\sin^2\left(\frac{b-1}{2}\varphi\right)}\,\mathrm{d}\varphi \\
&= |1+ab|\cdot\int_0^\phi \sqrt{1-\frac{4ab}{(1+ab)^2}\sin^2\left(\varphi\frac{b-1}{2}\right)}\,\mathrm{d}\varphi \\
&= \frac{2|1+ab|}{b-1}\cdot\mathrm{E}\left(\phi\frac{b-1}{2}\middle|\frac{4ab}{(1+ab)^2}\right) \qquad (3)
\end{aligned}$$

	$b=-1$	**Hypotrochoids** $b<0$	**Epitrochoids** $b>0$	$b=1$
Curtate $\lvert ab\rvert<1$	ellipse	curtate hypotrochoid	curtate epitrochoid	circle
Cycloid $\lvert ab\rvert=1$	Tusi couple	hypocycloid	epicycloid	circle
Prolate $\lvert ab\rvert>1$	ellipse	prolate hypotrochoid	prolate epitrochoid	circle

Table 1: Classification of trochoids and their names.

2.2 Incomplete elliptic integral of the second kind

Before we approximate the inverse of the incomplete elliptic integral of the second kind, let us review its properties.

$$\mathrm{E}(\phi|m) = \int_0^{\phi} \sqrt{1-m\cdot\sin^2\varphi}\,\mathrm{d}\varphi\ ,\ \phi\in[0,2\pi),\ m\in[0,1]$$

The complete elliptic integral of the second kind is $\mathrm{E}(m)=\mathrm{E}\left(\frac{\pi}{2}|m\right)$. Special values: $E(0|m)=0$, $E(\phi|0)=\phi$. The incomplete elliptic integral grows linearly and it is also 2π periodic, that is $\mathrm{E}(\phi|m)=\frac{2}{\pi}\mathrm{E}(m)\cdot\phi+\mathrm{E}(\phi \mod 2\pi\mid m)$. Moreover, we can tile the periodic part with the quarter period. For trochoids, we can calculate $E(\phi|m)$ for negative m values with $m\to\frac{m}{m-1}\in(0,1)$ using the following formula. A pair of these corresponding values of m are highlighted in Figure 4a where the incomplete elliptic integral is visualized.

Lemma 1. *For any $\phi\in\mathbb{R}$ and $0\neq m\in\mathbb{R}$,*

$$\mathrm{E}(\phi|m)=\sqrt{1-m}\left(\mathrm{E}\left(\tfrac{m}{m-1}\right)-\mathrm{E}\left(\tfrac{\pi}{2}-\phi|\tfrac{m}{m-1}\right)\right)\ . \quad (4)$$

Proof. Subtitute $\phi=\frac{\pi}{2}-\theta$ as if we rotated the trochoid by 90° degrees:

$$\begin{aligned}\mathrm{E}(\phi|m)&=\int_0^{\phi}\sqrt{1-m\sin^2\varphi}\,\mathrm{d}\varphi\\ &=\int_{\pi/2-\phi}^{\pi/2}\sqrt{1-m\cos^2\theta}\,\mathrm{d}\theta\\ &=\sqrt{1-m}\int_{\pi/2-\phi}^{\pi/2}\sqrt{1-\tfrac{m}{m-1}\sin^2\theta}\,\mathrm{d}\theta\\ &=\sqrt{1-m}\left(\mathrm{E}\left(\tfrac{m}{m-1}\right)-\mathrm{E}\left(\tfrac{\pi}{2}-\phi|\tfrac{m}{m-1}\right)\right)\end{aligned}$$

□

Lemma 2. *If $\xi\cdot\mathrm{E}(m)=\mathrm{E}(\phi|m)$ for any $\xi,\phi\in\mathbb{R}$ and $0\neq m\in\mathbb{R}$, then*

$$\phi=\frac{\pi}{2}-\mathrm{E}^{-1}\left(\mathrm{E}\left(\tfrac{m}{m-1}\right)(1-\xi)\ \middle|\ \tfrac{m}{m-1}\right)$$

Proof. Substitute $\xi\cdot\mathrm{E}(m)$ into the left side of Equation (4) and rearrange to obtain

$$\mathrm{E}\left(\tfrac{\pi}{2}-\phi\ \middle|\ \tfrac{m}{m-1}\right)=\mathrm{E}\left(\tfrac{m}{m-1}\right)-\frac{\mathrm{E}(m)}{\sqrt{1-m}}\cdot\xi\ .$$

Using the same Lemma 1 for $\theta=\frac{\pi}{2}$, we get the formula for the complete elliptic integral $\mathrm{E}(m)=\sqrt{1-m}\cdot\mathrm{E}\left(\frac{m}{m-1}\right)$ which when applied for the above leads to

$$\mathrm{E}\left(\tfrac{\pi}{2}-\phi\ \middle|\ \tfrac{m}{m-1}\right)=\mathrm{E}\left(\tfrac{m}{m-1}\right)-\mathrm{E}\left(\tfrac{m}{m-1}\right)\xi\ .$$

Rearranging the above completes the proof of Lemma 2. □

Figure 4 illustrates the geometry of the direct and inverse elliptic functions.

2.3 Simplifying $E^{-1}(\xi|m)$

Note that if $m<0$, Lemma 2 shows that we can remap into the $(0,1)$ range. Thus, let us now assume that $m\in[0,1],\xi\in[0,1)$ so we can compute $\theta\in[0,\frac{\pi}{2}]$ from

$$\theta=\mathrm{E}^{-1}\left(\mathrm{E}(m)\cdot\xi|m)\right)\ ,$$

provided we have a good approximation of the right-hand side over the $(\xi,m)\in[0,1]^2$ domain. To aid with the approximation, let us remove the linear term as in Figure 4b, square the function, and apply a $W(\xi,m)$ weight function:

$$\left(\mathrm{E}^{-1}\left(\mathrm{E}(m)\xi\,|\,m\right)-\frac{\pi}{2}\xi\right)^2\approx W(\xi,m)\cdot G(\xi,m),\quad (5)$$

$$W(\xi,m)=\frac{m\cdot\xi\cdot(1-\xi)}{\sqrt{2-\xi-m}}\ ,\quad (6)$$

where $G(\xi,m)$ is the function we approximate with. The weight function is used to smooth out the pole in the derivative at $(\xi,m)=(1,1)$ and zero out the function at $m=0$, $\xi=0$, or $\xi=1$ values where it should be zero. Figure 5a visualizes this approximation problem.

The computation of $G(\xi,m)$ can be carried out in multiple ways, but we found the above transformations helped the most to obtain a higher precision low-rank and low-degree approximation.

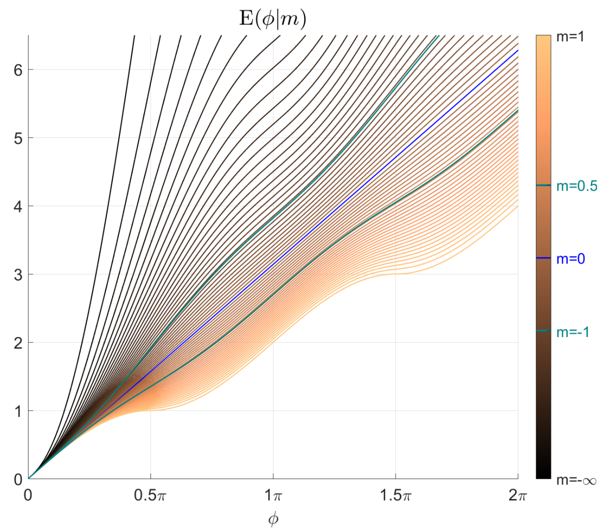

(a) $\theta \mapsto \mathrm{E}(\theta|m)$ functions for $m \in (-\inf, 1]$. Lemma 1 relates the $m = 0.5$ and $m = -1$ teal curves.

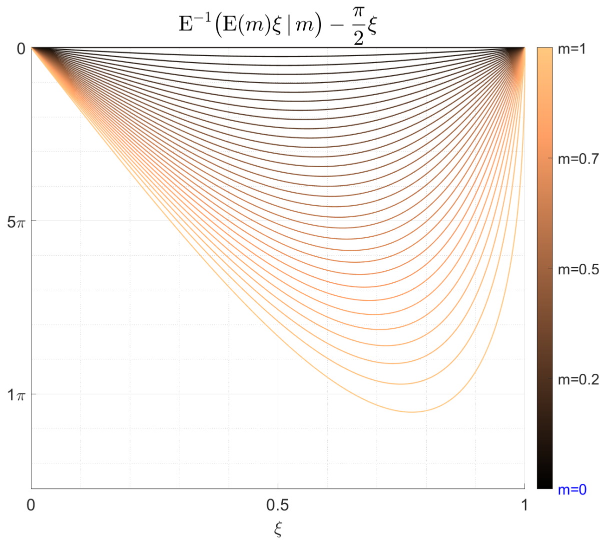

(b) $\xi \mapsto \mathrm{E}^{-1}\left(\mathrm{E}(m)\xi|m\right) - \frac{\pi}{2}\xi$ functions for various $m \in [0, 1]$ values show the deviation from the linear function.

Figure 4: The incomplete integral of the second kind and its modified inverse that we need to approximate.

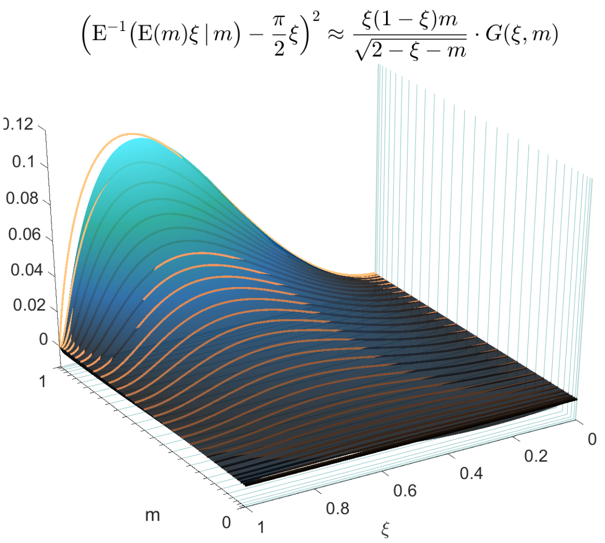

(a) Transformed incomplete elliptic inverse orange curves approximated with the blue surface with weight function.

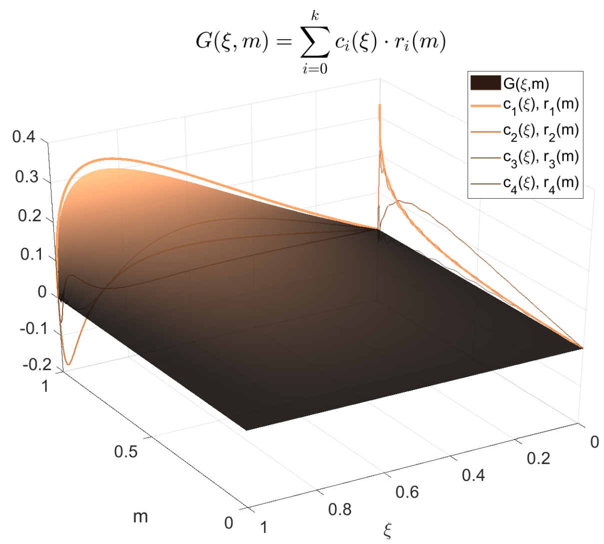

(b) Low-rank component functions of the transformed inverse incomplete elliptic integral.

Figure 5: Transformation and low-rank approximation of the inverse elliptic integral of the second kind

3 LOW-RANK APPROXIMATION

We want to find a k-rank approximation first, that is, a pair of c_i and r_i functions such that

$$G(\xi, m) = \sum_{i=0}^{k} c_i(\xi) \cdot r_i(m) \qquad c_i, r_i : [0,1] \to \mathbb{R} \quad (7)$$

Figure 5b visualizes the $G(\xi, m)$ function with $c_i(\xi)$ and $r_i(m)$ component functions drawn on the back walls. If we evaluate the functions in Equation (5) at $\xi_1, \ldots, \xi_M$ and $m_1, \ldots, m_N$ values to get the matrix of function values we want G to reproduce, we can perform a k-rank Singular Value Decomposition (SVD), that is,

$$G = UDV^{\mathsf{T}}, \qquad U \in \mathbb{R}^{M\times k}, D \in \mathbb{R}^{k\times k}, V \in \mathbb{R}^{N\times k}$$

where we just have to find c_i and r_i functions that reproduce the i-th column of $U \cdot \sqrt{D}$, and $V \cdot \sqrt{D}$ matrices to extend G as a function with Equation (7). More specifically, for $i = 1, \ldots, k$, $j = 1, \ldots, M$, and $l = 1, \ldots, N$:

$$c_i(\xi_j) \approx U_{ji}\sqrt{|D_{ii}|},$$
$$r_i(m_l) \approx V_{li}\,\mathrm{sgn}\,D_{ii}\sqrt{|D_{ii}|}\,.$$

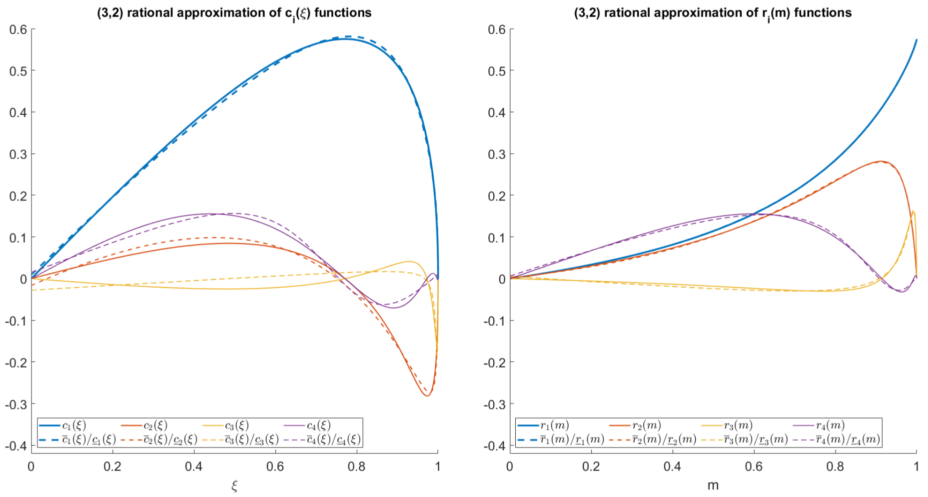

Figure 6: Component functions $c_i(\xi), r_i(m)$ and their rational approximations $\frac{\overline{c_i}(\xi)}{\underline{c_i}(\xi)}$ and $\frac{\overline{r_i}(m)}{\underline{r_i}(m)}$ where the nominator polynomials are cubic, and the denominators are quadratic.

Figure 5 illustrates the transformation of the elliptic inverse integral and its decomposition into a low-rank approximation. Figure 6 shows the component functions of an approximation.

4 RATIONAL POLYNOMIAL APPROXIMATION

To approximate the above c_i and r_i functions at ξ_j and m_l values, we can apply low-degree rational polynomial approximations to find $\overline{c_i}$, $\underline{c_i}$, $\overline{r_i}$, and $\underline{r_i}$ polynomials.

$$\begin{aligned} G(\xi,m) &= \sum_{i=0}^{k} c_i(\xi)\cdot r_i(m) \\ &= \sum_{i=0}^{k} \frac{\overline{c_i}(\xi)}{\underline{c_i}(\xi)} \cdot \frac{\overline{r_i}(m)}{\underline{r_i}(m)} \end{aligned} \tag{8}$$

For these last steps, we employed the Chebfun Matlab library [Dri14] for their state-of-the-art polynomial approximation algorithms. Figure 7 plots the error of a degree $(3,2)$ and rank 3 approximation.

5 RESULTS

Let us consider finding a separable $(2,1)$ rational approximation solution to the arc-length parametrization problem of trochoids using Matlab and Chebfun. Since Chebfun relies on the Chebyshev basis, our sample points are on the Chebyshev grid of

$$\xi_j = -\cos\left(\pi\frac{j-1}{M-1}\right), \qquad m_l = -\cos\left(\pi\frac{l-1}{N-1}\right),$$

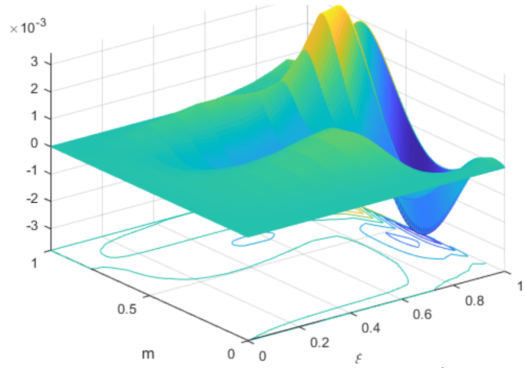

Figure 7: $W(\xi,m)\cdot G(\xi,m) - W(\xi,m)\cdot \widehat{G}(\xi,m)$ approximation error for a 3-rank and (3,2)-degree decomposition.

for $j = 1,\ldots,M$ and $l = 1,\ldots,N$. The resulting approximation is

$$\begin{aligned} \widehat{G}(\xi,m) &= \frac{\xi^2 - 0.9553\cdot\xi - 0.04578}{1.539\cdot\xi - 1.5626} \\ &\quad\cdot \frac{m^2 + 0.3193\cdot m - 0.09471}{-23.993\cdot m + 26.213} \\ \widehat{E}(m) &= \frac{m^2 - 5.5788\cdot m + 5.3188}{-2.6429\cdot m + 3.3811} \end{aligned} \tag{9}$$

Figure 8 illustrates the error of this approximation compared to the exact arc-lengths for trochoids corresponding to $a = 1$ and $b = 1, 2, \ldots, 16$. The error is within $3\cdot 10^{-3}$ even at the arc-length of 60.

To evaluate our explicit approximate natural parameterization for any (a,b) trochoid at any $s \in \mathbb{R}$ parameter, we derive the inverse arc-length function from Eq. (3):

$$s_{\boldsymbol{p}}^{-1}(s) = \frac{2}{b-1}\cdot \mathrm{E}^{-1}\left(s\frac{b-1}{2|1+ab|}\,\middle|\,\frac{4ab}{(1+ab)^2}\right). \tag{10}$$

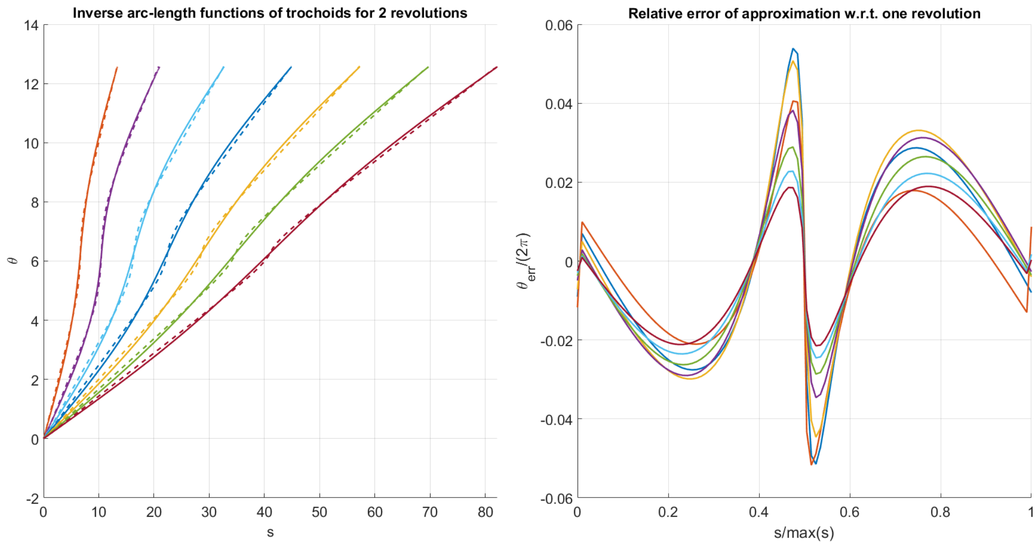

Figure 8: Precise $s_{\boldsymbol{p}}^{-1}$ compared to 1-rank separable (2,1)-degree rational approximation for trochoids with $a = 1, 3 \ldots, 13$, and $b = 0.5$. Albeit the error is not small, the approximation here is a crude quadratic over linear rational separable approximation using the code seen in Fig. 9. Note that only one global approximation is needed to evaluate the arc-lengths of any trochoid.

Therefore, we can calculate

$$\xi := \frac{s}{\widehat{E}(m)} \frac{b-1}{2|1+ab|}, \; m := \frac{4ab}{(1+ab)^2} . \tag{11}$$

Since the approximant below has a period of 4 and a quarter period of 1 that we can tile with, that is

$$E^{-1}\left(\mathrm{E}(m)(2-\xi)|m\right) = \pi - E^{-1}\left(\mathrm{E}(m)\xi|m\right) .$$

Assuming $\xi \in [0,1]$, we compute $\widehat{G}$ with Eq. (8), for example with Eq. (9). Finally, evaluate $W(\xi, m)$ and $E^{-1}(s|m)$ which is obtained from Eq. (5) as

$$\mathrm{E}^{-1}\left(\mathrm{E}(m)\xi\,|m\right) = \frac{\pi}{2}\xi - \sqrt{W(\xi,m)\cdot G(\xi,m)} . \tag{12}$$

Figure 9 provides an example implementation for a purely separable approximation $g(\xi,m) = c(\xi) \cdot r(m)$ where the $c(\xi)$, $r(m)$, $E(m)$ functions are approximated with $(2,1)$ rational polynomials.

6 CONCLUSIONS

We derived an algorithmic framework to compute high-accuracy approximate trochoid natural parametrizations. This family of curves includes circles, ellipses, and a variety of well-known shapes.

We demonstrated that our formulation may be used to derive low-degree rational polynomial parametrizations that approximate unit-speed traversal. Nevertheless, for optimal results, we had to apply an appropriate simplification and weighting of the approximated function.

Even though we restricted the number of degrees of freedom to two by choice of trochoids, our construct may be generalized to higher dimensions, in other words, to curves of higher flexibility; this is a future research direction.

ACKNOWLEDGMENTS

Supported by the ÚNKP-22 New National Excellence Program of the Ministry for Innovation and Technology from the source of the National Research, Development and Innovation Fund.

REFERENCES

[BHS87] Carl de Boor, Klaus Höllig, and Malcolm Sabin. “High accuracy geometric Hermite interpolation”. In: *Computer Aided Geometric Design* 4.4 (Dec. 1987), pp. 269–278. ISSN: 0167-8396. DOI: 10.1016/0167-8396(87)90002-1.

[Car18] Manfredo Perdigão do Carmo. *Differential geometry of curves & surfaces*. Revised & updated second edition. Mineola, New York: Dover Publications, INC, 2018. ISBN: 978-0-486-80699-0.

[Dri14] Trefethen Driscoll Hale. *Chebfun Guide*. Oxford: Pafnuty Publications, 2014.

[Far08] Rida T. Farouki. *Pythagorean-Hodograph Curves: Algebra and Geometry Inseparable*. Ed. by Herbert Edelsbrunner, Leif Kobbelt, and Konrad Polthier. Vol. 1. Geometry and Computing. Berlin, Heidelberg: Springer Berlin Heidelberg, 2008. ISBN: 978-3-540-73398-0. DOI: 10.1007/978-3-540-73398-0.

[Far97] Rida T. Farouki. “Optimal parameterizations”. In: *Computer Aided Geometric Design* 14.2 (Feb. 1997), pp. 153–168. ISSN: 01678396. DOI: 10.1016/S0167-8396(96)00026-X.

```matlab
function [theta] = trochoidInverseArclength(s, a, b, Ep, Eq, Cp, Cq, Rp, Rq)
    % Approximate inverse arc-length function of trochoids from Eq. (2)
    arguments
        s  (1,:) double                  % distance taken on trochoid parameterized as:
        a  (1,1) double                  % p(t) = [ cos(t) + a*cos(b*t) ,
        b  (1,1) double                  %          sin(t) + a*sin(b*t) ].
        Ep (1,:) double = [ 1   -5.5788    5.3188 ]  % Rational approx of the complete integral
        Eq (1,:) double = [     -2.6429    3.3811 ]  % E(m) ~= Ep(m)/Eq(m)
        Cp (1,:) double = [ 1   -0.9544   -0.0481 ]  % overlined  c(xi) polynom in the paper
        Cq (1,:) double = [      1.2038   -1.2610 ]  % underlined c(xi) polynom in the paper
        Rp (1,:) double = [ 1   -3.5267    0.0720 ]  % overlined  r(m)  polynom in the paper
        Rq (1,:) double = [     16.2103  -20.5069]   % underlined r(m)  polynom in the paper
    end

    m = 4*a*b/(1 + a*b + 1e-12).^2;                      % m from a,b in Eq. (3)
    xi = 0.5*(b-1) / ((abs(1+a*b)+1e-12) * E(m)) * s;    % xi from Eq. (11)
    theta = 2/(b-1) * Einv(xi, m) ;                      % s^{-1}(s) from Eq. (10)

    function e = E(m)
        % Approximation of the complete elliptic integral of the second kind
        e = 1;
        if m < 0
            e = sqrt(1-m); % Extending to m < 0 with Lemma 1 for the complete elliptic
            m = m/(m-1);   % We turn negative m values to be in [0,1] with Eq. (4)
        end
        e = e * polyval(Ep, m) ./ polyval(Eq, m); % Rational approximation
    end

    function einv = Einv(xi,m)
        % Approximation of the inverse of the incomplete elliptic integral of the second kind
        is_m_neg = m < 0;
        if is_m_neg
            xi = 1-xi;       % We extend to m < 0 with Lemma 2 for the inverse elliptic
            m = m/(m-1);     % We turn negative m values to be in [0,1]
        end

        xi2 = mod(xi,2);     % Remap xi from [-inf,inf] to [0,2].
        xi1 = 1-abs(xi2-1); % Remap xi from [0,2] to [0,1]. Sign fixed in line 4

        g =  polyval(Cp,xi1) .* polyval(Rp,m) ...          % Seperable rational approximation
         ./ (polyval(Cq,xi1) .* polyval(Rq,m));            % of G(xi,m) from Eq. (8)
        einv = 0.5*pi*xi - sign(1-xi2).*g;  % Linear + perioid term in Eq. (12)

        if is_m_neg
            einv = 0.5*pi - einv;    % If m was negative, we use Lemma 2.
        end
    end
end
```

Figure 9: This simplified Matlab code example evaluates approximate arc-length functions, omitting the weight function calculation.

[FS07] Rida T. Farouki and Takis Sakkalis. "Rational space curves are not "unit speed"". In: *Computer Aided Geometric Design* 24.4 (May 2007), pp. 238–240. ISSN: 01678396. DOI: 10.1016/j.cagd.2007.01.004.

[Jüt97] Bert Jüttler. "A vegetarian approach to optimal parameterizations". In: *Computer Aided Geometric Design* 14.9 (Dec. 1997), pp. 887–890. ISSN: 01678396. DOI: 10.1016/S0167-8396(97)00044-7.

[SC15] J. Sánchez-Reyes and J. M. Chacón. "A polynomial Hermite interpolant for C2 quasi arc-length approximation". en. In: *Computer-Aided Design* 62 (May 2015), pp. 218–226. ISSN: 0010-4485. DOI: 10.1016/j.cad.2014.12.001.

[Sch98] Robert Schaback. "Optimal Geometric Hermite Interpolation of Curves". In: (1998). Accepted: 2023-02-16T13:21:53Z Publisher: Vanderbilt U. Press.